# Intermetallic Compounds in Solder Alloys: Common Misconceptions

# Dave Hillman<sup>1</sup>, Tim Pearson<sup>2</sup>, Richard Coyle<sup>3</sup>

<sup>1</sup>Hillman Electronic Assembly Solutions, LLC Cedar Rapids, IA, USA

> <sup>2</sup>Collins Aerospace Cedar Rapids, IA, USA

³Nokia Murray Hill, NJ, USA

## **ABSTRACT**

The Intermetallic compounds (IMC) or intermediate phases are formed between two or more metallic elements in many metal alloy systems. During soldering, an IMC is formed at the soldered interface as the molten solder reacts with an element in the substrate. IMCs also can form within the bulk solder as the joint solidifies. IMCs have critical roles in the solder joint quality and reliability. Unlike most metal alloys, an intermetallic compound typically has a fixed stoichiometry and is in variance with the conventional phases or constituents in the metal system (e.g., alpha and beta). IMCs have a different crystal structure than any of its constituents and some but never all the characteristics and properties of its constituents. Ductility is an important solder joint property, and the low intrinsic ductility of IMCs is associated with brittle behavior and reliability risk in service. However, a review of published solder field failures shows little evidence that IMC properties or IMC evolution under service conditions reduce solder joint reliability. Most IMC-induced solder joint failures are found to result from incorrect material specification or uncontrolled soldering processes. This paper describes the IMCs that occur typically in eutectic, Sn63Pb37 solder and near-eutectic SAC305 or other tin-based Pb-free solder alloys, including how they impact solder joint reliability. The paper also describes the potential impact of IMCs on the solder joint reliability for the newest generation of Pb-free high-performance solder alloys.

Key Words: Intermetallic Compound (IMC), tin/lead solder, Pb-free solder

# **INTRODUCTION**

In soldering, an IMC is formed by the reaction of the molten solder with the substrate and is a critical element in solder joint reliability. The thickness of this metallurgical bond increases with

the time the molten solder is in contact with the substrate being soldered. Tin based solder alloys form an IMC thickness that is typically 1-3 µm for most soldering processes used in the printed circuit assembly processes [1]. The IMC thickness increases as the solder joint ages in the solder state. The physical properties of IMCs are typically quite different than the solder and substrate materials. In general IMCs are stronger and have lower ductility (aka being more brittle) which can have an effect on the overall solder joint reliability. Excessive IMC thickness due to incorrect or out of control soldering processes can become a crack initiation region during the deformation of a solder joint. Although solder alloys are regarded as ductile materials, they can exhibit brittle physical properties under certain conditions. Figure 1 illustrates how a variety of solder alloys all undergo have ductile to brittle behavior with decreasing temperature. IMC phases can also be found in the solder microstructure matrix where they can affect the solder joint microstructure and properties.

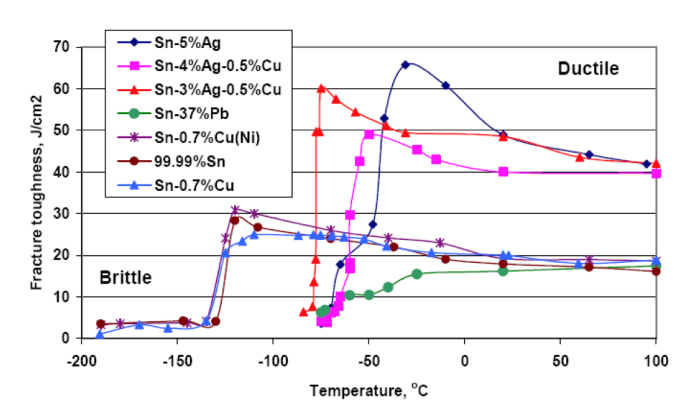


Figure 1: Solder Alloy Ductile to Brittle Behavior [2]

## **IMCS IN SNPB SOLDER ALLOYS**

Copper is one of the most widely used substrate surfaces used in the formation of solder joints. The identification of specific IMC phases is accomplished using phase diagrams. In tin-based solder alloys, two IMCs are formed - Cu<sub>6</sub>Sn<sub>5</sub> and Cu<sub>3</sub>Sn (shown in Figure 2 as η' phase and γ phase respectively). The Cu<sub>6</sub>Sn<sub>5</sub> IMC forms during the initial formation of the solder joint. The Cu<sub>3</sub>Sn IMC phase forms over time as the Cu<sub>6</sub>Sn<sub>5</sub> IMC phase creates a diffusion barrier slowing the movement of the copper atoms. Figure 3 illustrates both the Cu<sub>6</sub>Sn<sub>5</sub> and Cu<sub>3</sub>Sn IMC phases after solder joint formation and thermal cycling. The Cu<sub>6</sub>Sn<sub>5</sub> IMC phase is also commonly found in the solder joint microstructure formed during the solder joint formation (Figure 4). The IMC thickness formed in most soldering processes is between 1 and 3 μm [1].

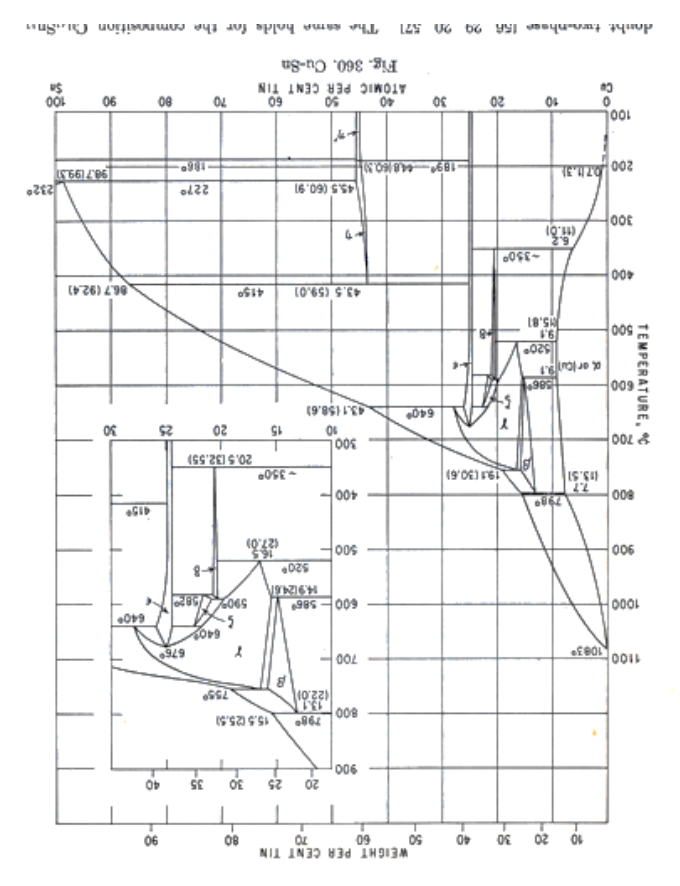


Figure 2: Copper Tin Phase Diagram [3, 4]

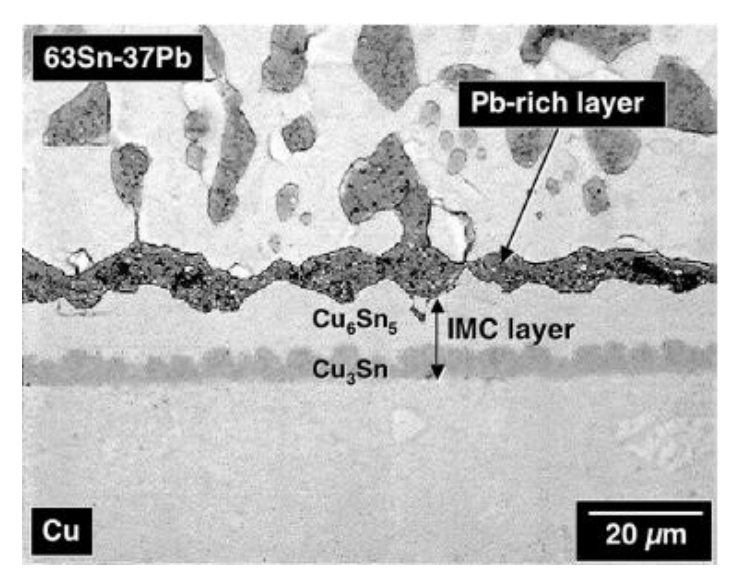


Figure 3: Copper Tin IMC Phases in SnPb Solder [5]

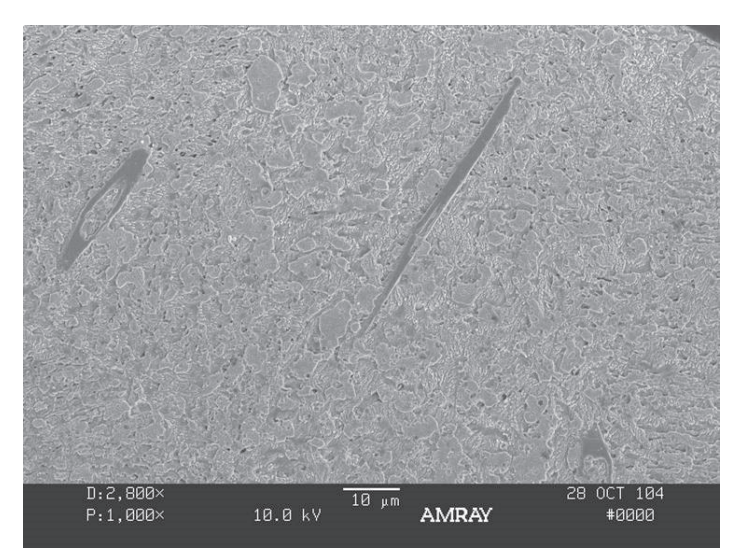


Figure 4: Large  $Cu_eSn_s$  IMC Phase Needles Observed in a SnPb Solder Joint [6]

The use of nickel as a solderable substrate in Sn based solder alloys, primarily found with the use of electroless nickel/immersion gold (ENIG) printed circuit board finishes and in ball grid array (BGA) pad surface finishes, results in the formation of Ni3Sn4 IMC phase (Figure 5). Figure 6 illustrates the Ni3Sn4 IMC phase at the solder joint/substrate interface.

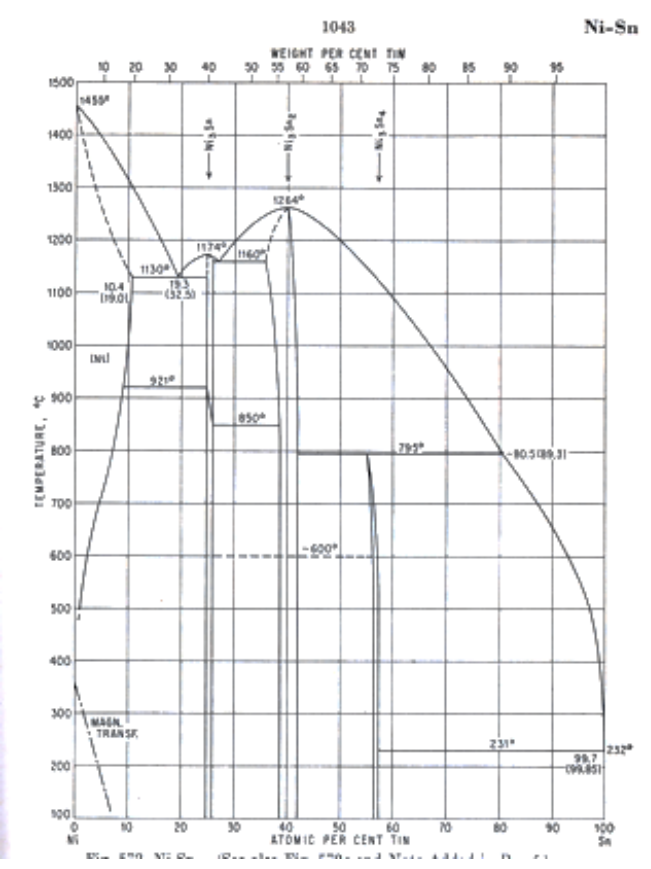


Figure 5: Tin Nickel Phase Diagram [3,4]

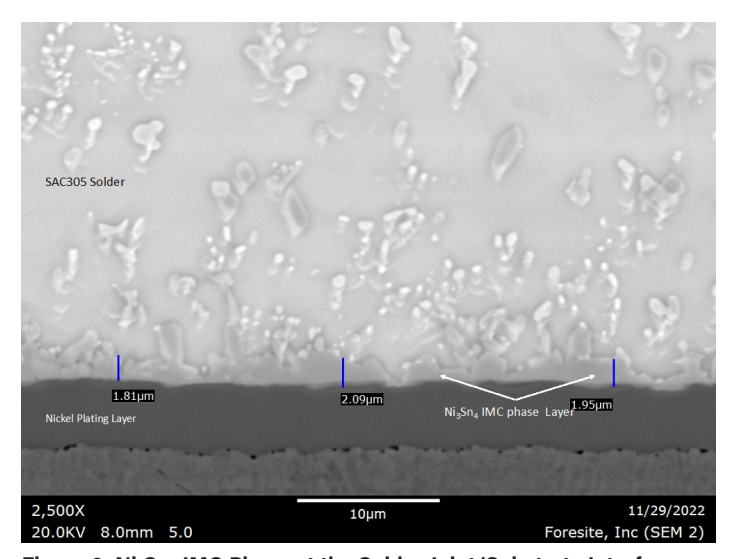


Figure 6:  $Ni_3Sn_4$  IMC Phase at the Solder Joint/Substrate Interface (Photo courtesy of Terry Munson, Foresite)

# **IMC PHASES IN SAC SOLDER ALLOYS**

The Sn-based SAC alloys form the same copper IMC phases (Cu<sub>6</sub>Sn<sub>5</sub>, Cu<sub>3</sub>Sn) as discussed in the SnPb solder alloy section. Hodulova et.al. [7], using thermal aging processing post soldering, determined that the Cu<sub>6</sub>Sn<sub>5</sub> phase formed during the soldering

process and the Cu<sub>3</sub>Sn phase formed during thermal aging. The Cu<sub>3</sub>Sn phase thickness was limited by the Cu<sub>6</sub>Sn<sub>5</sub> phase acting as a diffusion inhibitor. The copper IMC phases growth and thicknesses are sensitive to the higher copper concentrations found in the Sn-based SAC alloys.

In addition to the copper and nickel-based IMC phases discussed, the Sn-based, SAC alloys have silver-tin IMC phases too, since they utilize Ag as a primary constituent element addition. The tin/silver phase diagram (Figure 7) shows solubility of Ag in Sn of less than 0.1 wt. % up to 200°C (Ag<sub>3</sub>Sn IMC indicated as ζ phase). During solidification of SAC solders, the Ag and Sn react to form networks of Ag<sub>3</sub>Sn precipitates at the primary Sn dendrite boundaries (Figure 8).

ence of the  $\zeta$  phase, first detected by potential measurements [14] and gennitely established by thermal and micrographic studies [4], was confirmed by X-ray investi-

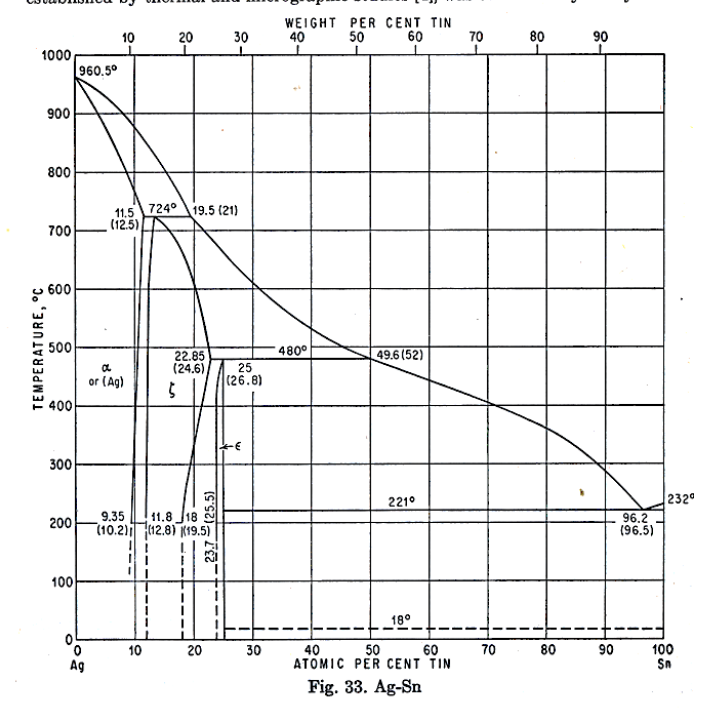


Figure 7: Silver/Tin Phase Diagram [3,4]

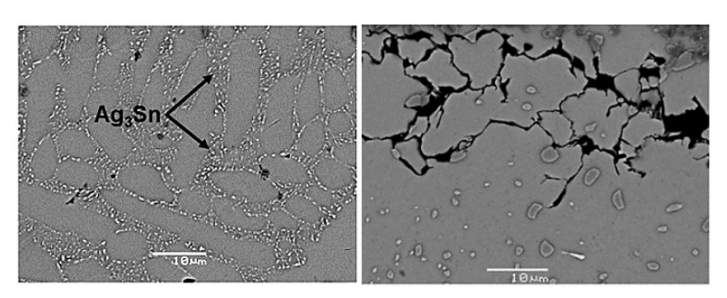


Figure 8: Backscattered scanning electron micrographs illustrating Ag<sub>3</sub>Sn IMC Phase in SAC305: As Solidified (left), After Thermal Cycling [8]

# Gold IMC In SnPb and SAC Solder Alloys

Gold plating is used as a solderable surface finish for both components and printed circuit boards in the electronics industry for decades. Gold is primarily plated over nickel, to prevent the formation of nickel oxide which has extremely poor solderability characteristics. Gold surface finish plating provides three distinct attributes: (1) gold is an excellent electrical contact surface due to its low electrical resistance and good solderability, (2) gold does not form an oxide layer which leads to maintenance of excellent solderability during storage, and therefore is often considered the optimal surface finish for printed circuit board and components in long-term storage, and (3) gold is used as a sacrificial surface finish rather than a primary solder finish, as it dissolves into the solder leaving behind a pristine surface of the underlying nickel layer to which the solder wets to and reacts, forming a solder-nickel interface in the solder joint. Figure 9 depicts the tin/gold phase diagram shows solubility of Au in Sn of less than 0.3 wt. % from room temperature to 200°C.

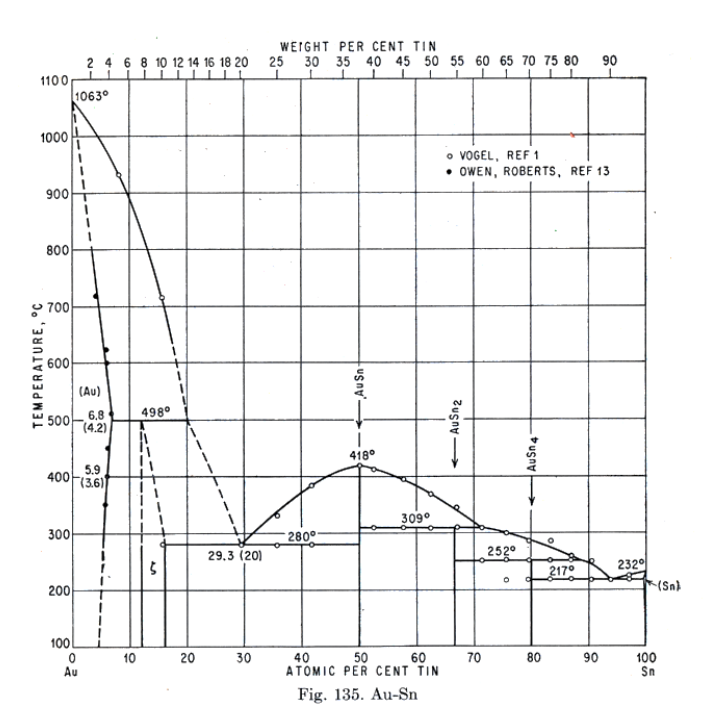


Figure 9: Gold/Tin Phase Diagram [3,4]

Bader documented the dissolution rate of gold into a 60Sn40Pb solder alloy recording a dissolution rate of approximately 1  $\mu$ m/second at 200°C [9]. Hillman et al. documented the dissolution rate of gold in SAC305 solder of approximately 6  $\mu$ m/second at 250°C [10]. Figure 10 and Figure 11 show the differences of gold dissolution rate compared with other metals in SnPb and SAC305 solder alloys. The high solubility and fast dissolution rates of gold in molten solder make it well suited as a sacrificial surface finish for both SnPb and Pb-free soldering processes.

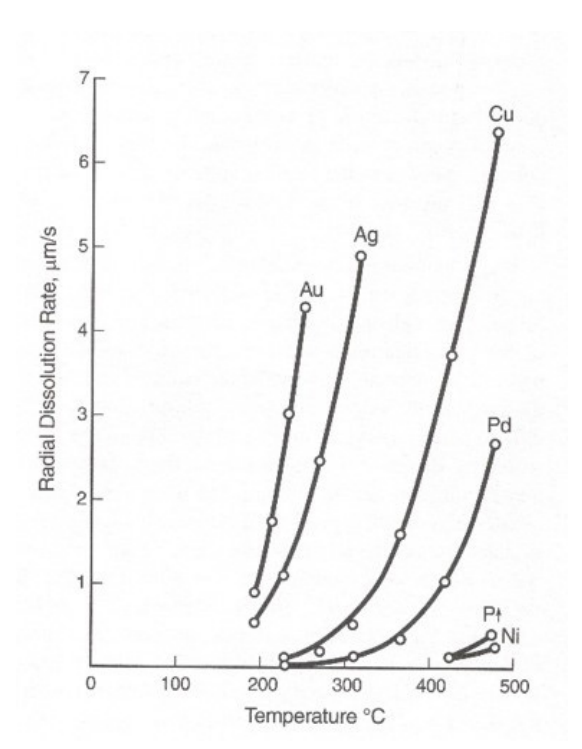


Figure 10: Dissolution Rates of Various Elements in 60Sn40Pb Solder [9]

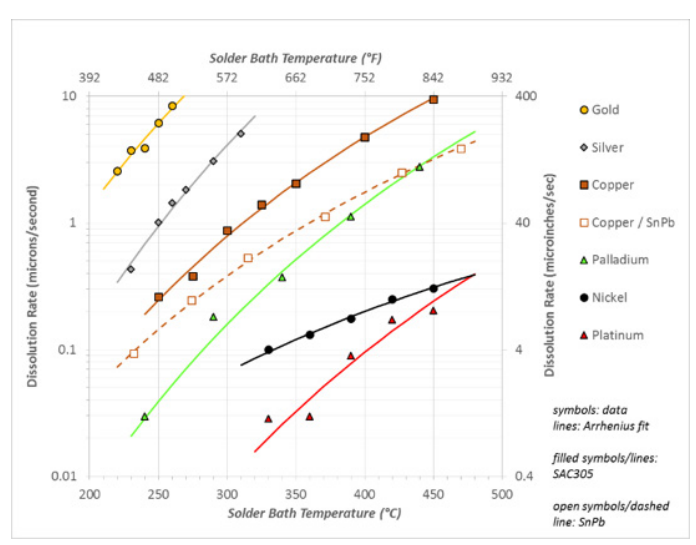


Figure 11: Dissolution Rates of Various Elements in SAC305 Solder compared with Cu dissolution into SnPb [10] Note that the vertical scale (dissolution rate) is a log scale

The AuSn<sub>4</sub> IMC phase forms as high-aspect ratio platelets in solder joints. Figure 12 illustrates the AuSn<sub>4</sub> morphology as a platelet structure in a SnPb solder joint. When the gold concentration in the solder joint exceeds approximately 3-5% by weight, the elongated platelets form and influence the solder joint reliability. Figure 13 is a scanning electron microscopy image showing AuSn<sub>4</sub> IMC platelets.

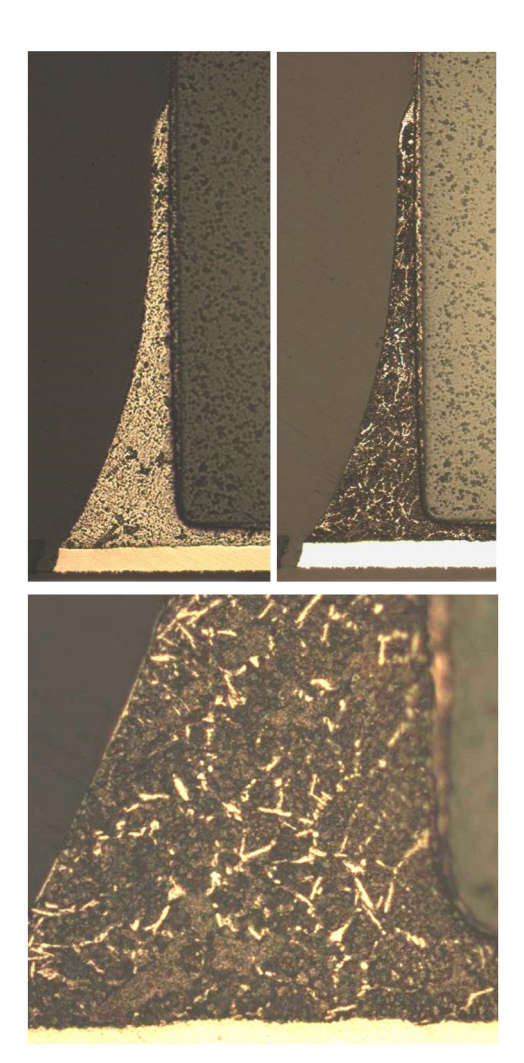


Figure 12: Optical photomicrograph of a solder joint containing AuSn<sub>4</sub> IMC phase (white platelets). Upper left, as polished, Upper right, Carapella's reagent, Lower center - higher magnification of etched sample (Photos courtesy of Collins Aerospace).



Figure 13: Scanning electron microscopy image of etched Sn-Pb solder joint containing AuSn<sub>4</sub> IMC platelets (Photo courtesy of Collins Aerospace)

The origin of the 3-5wt% Au limit comes from Bester who conducted IZOD impact testing demonstrating the effect of the amount of gold/tin intermetallic phase on the solder joint integrity as a function of the gold content of the solder joint up to 10 wt.% Au [11]. As shown in Figure 14, Bester's test results show a pronounced IZOD test data impact, with compositions less than approximately 4 wt.% Au content show a small drop in performance but with a pronounced drop in performance at 5wt% Au. These results demonstrated that a small fraction of AuSn<sub>4</sub> platelets in the solder joint microstructures (below 3-4wt% Au) do not degrade the solder joint integrity as measured by impact testing. Solder joint integrity degrades in the 3- 5wt% Au range.

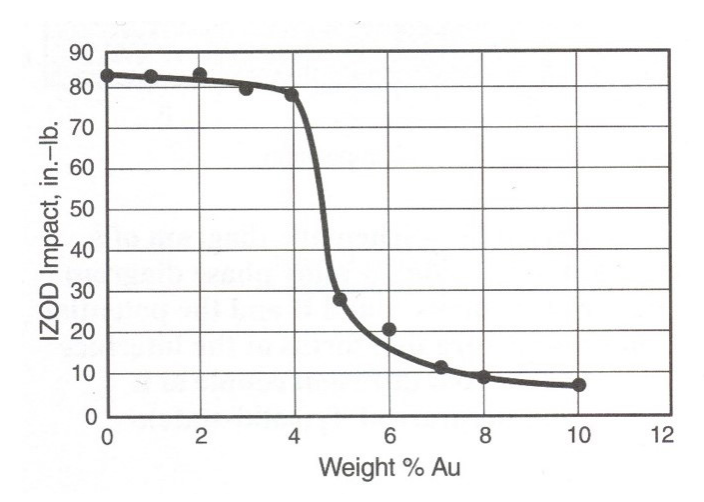


Figure 14: Bester's IZOD impact test data as a function of gold concentration [11]

### Palladium IMC In SnPb and SAC Solder Alloys

Palladium and tin form a brittle intermetallic phase in both SnPb and SAC solder alloys, PdSn<sub>4</sub>, which causes the degradation of solder joint integrity in a similar mode as gold/tin IMC phases. The PdSn<sub>4</sub> phase forms as platelets in the solder joint when the palladium concentration in the solder joint exceeds approximately 0.3%-1.0% by weight (Figure 15). The primary difference between palladium and gold is the diffusion rate into molten solder. As shown in Figure 11, the dissolution rate of palladium is orders of magnitude slower than gold and can potentially result in an increased risk of embrittlement. Industry investigations [12, 13, 14] have reported the formation of the brittle PdSn<sub>4</sub> intermetallic phase for palladium plating thicknesses in the 20-30 microinch range. Palladium finishes with thicknesses less than 20 micro inches have been shown not impact solder joint thermal cycle integrity [12, 15].

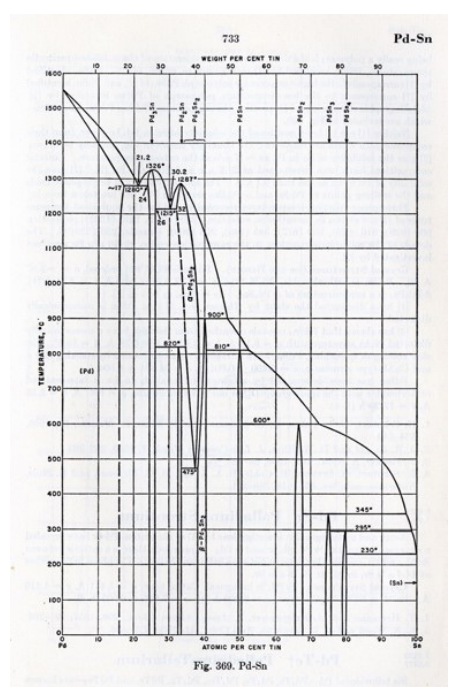


Figure 15: Palladium/Tin Phase Diagram [3,4]

#### **IMCS IN GENERATION 3 LEAD-FREE SOLDER ALLOYS**

# Metallurgical Considerations

The addition of Ag strengthens Sn and improves the creep resistance of the SAC solder by precipitation hardening as illustrated in Figure 8. The addition of other alloying elements can improve the creep resistance of the solder by means of two other well-known metallurgical strengthening mechanisms, solid solution hardening and dispersion hardening. The introduction of solute atoms into solid solution of a solvent-atom lattice invariably produces an alloy that is stronger than the pure metal [16]. Figure 16 shows a simplified schematic illustration of substitutional solid solution strengthening. Substitutional or interstitial solute atoms strain the lattice and dislocation movement, or deformation is inhibited by interaction between dislocations and solute atoms incorporated into the  $\beta$ -Sn lattice.

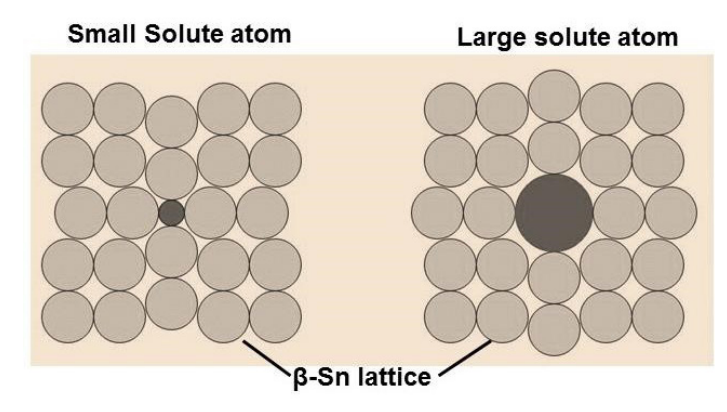


Figure 16: A simple schematic illustrating lattice distortion due to substitutional solute atoms.

If solute atoms precipitate from solution during thermal excursions in service, the solder alloy may strengthen subsequently due to dispersion hardening. Dispersion strengthening occurs when insoluble particles are finely dispersed in a metal matrix. Typical dispersion strengthened alloys employ an insoluble, incoherent second phase that is thermally stable over a large temperature range (Figure 17) [17]. For Sn-based solder alloys, the strength would be derived from a combination of increased solid solution strengthening at higher temperatures due to increased solubility, and dispersion strengthening that would supplement the solid solution effect at lower temperatures where solubility has decreased.

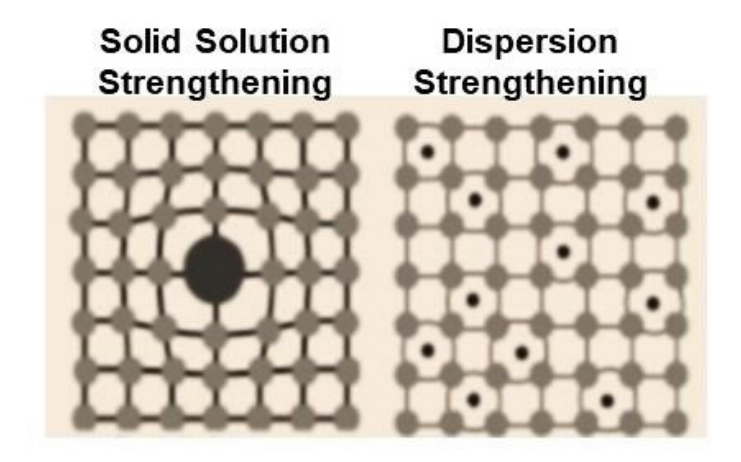


Figure 17: A simple schematic illustrating solid solution (left) and dispersion strengthening (right).

The development of Innolot provides evidence that substitutional solid solution strengthening can improve resistance to creep and fatigue at higher temperatures in Sn- based, Pb-free solders [18]. The current working hypothesis is that solid solution and dispersion strengthening not only supplement the Ag<sub>3</sub>Sn precipitate hardening found in SAC solders but continue to be effective once precipitate coarsening reduces the effectiveness of the intermetallic Ag<sub>3</sub>Sn precipitates [19].

The elements proposed most for improving elevated temperature properties in Sn-based, third generation solders are Bi, Sb and In. Bi and In, when used as a major alloying elements, also reduce the melting point of most solder alloy formulations, while the addition of Sb tends to increase the melting point [20]. These modified SAC alloys are off-eutectic compositions and are characterized by non-equilibrium solidification and often significant melting ranges [21-23].

# Antimony (Sb) Additions to Tin (Sn)

The binary Sn-Sb phase diagram in Figure 18 shows solubility of Sb in Sn of approximately 0.5 wt. % at room temperature to 1.5 wt. % at 125°C. Thus, some contribution is expected from solid solution strengthening due to Sb dissolved in Sn-based Pb-free solders [18].

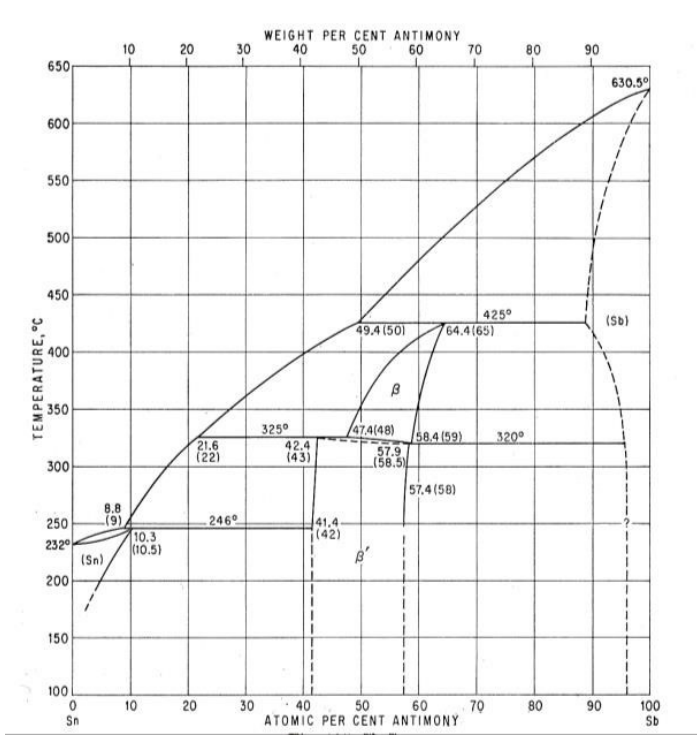


Figure 18: The Sn-Sb binary phase diagram [3,4]

Alloying with Sb may improve performance through other strengthening mechanisms. Studies by Li et al show that Sb slows the growth rate of Cu<sub>6</sub>Sn<sub>5</sub> intermetallic compound (IMC) layers at attachment interfaces [24, 25]. Fast interfacial IMC growth on Cu surfaces tends to produce irregular and non-uniform IMC layers. This can lead to reduced mechanical reliability by inducing fractures at IMC interfaces or through the IMC in drop/shock loading [26].

Figure 18 also shows that Sb has the potential to form multiple different intermediate phases or IMCs with Sn (Sb<sub>2</sub>Sn<sub>3</sub>, SbSn, Sb<sub>4</sub>Sn<sub>3</sub>, Sb<sub>5</sub>Sn<sub>4</sub>, and SbSn<sub>2</sub>) in the bulk solder. Lu et al [27] and El-Daly et al [28] identified SnSb intermediate phase precipitates <5µm in size and distributed throughout the Sn dendrites. Beyer et al show that Sn5Sb and Sn8Sb alloys have increased shear strength and ductility compared to conventional SAC solders and maintain their shear strength with good ductility after isothermal aging [29]. El-Daly suggests Sb also can improve creep performance and tensile strength [30]. In this case, the SbSn precipitates form within the Sn dendrites, unlike the well-known SAC Ag<sub>3</sub>Sn mechanism, where the precipitates form at the Sn dendrite boundaries. The SbSn precipitates work to resist recrystallization by strengthening the Sn dendrites [16].

# Indium (In) Additions to Tin (Sn)

The binary Sn-In phase diagram in shown in Figure 19. While there is disagreement over the solid solubility of In in Sn, a reasonable estimate is ~7 wt. % at room temperature and as much as 12 wt. % at 125°C [3,4]. Because of its range of solubility in Sn, In has been explored as a solid solution strengthening agent in Sn-based Pb-free solders [31-32]. The equilibrium diagram shows that

In forms two intermediate phases ( $\beta$  and  $\gamma$ ) of variable composition with Sn [3,4] but does not appear to form any true stoichiometric compounds with Sn.

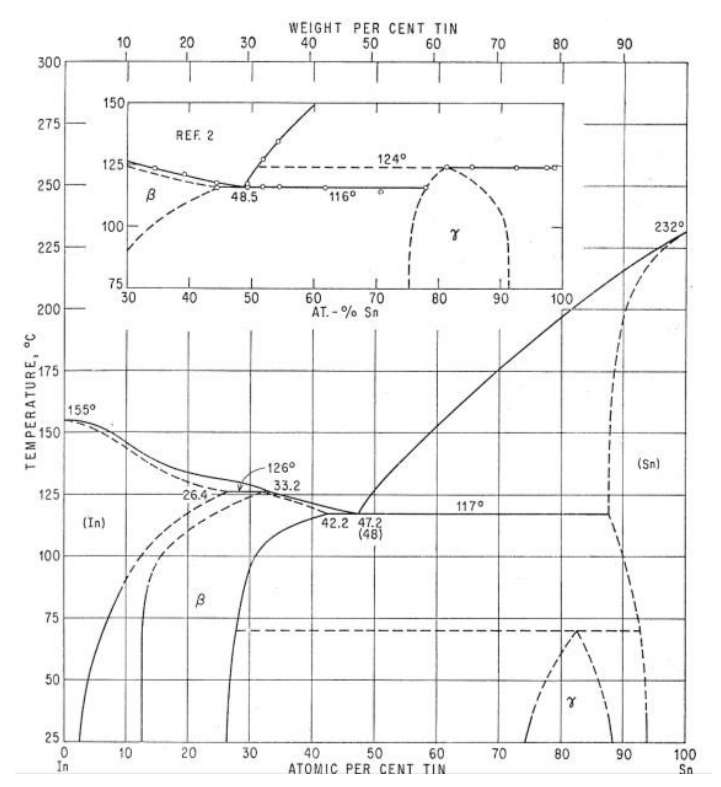


Figure 19: The In-Sn binary phase diagram [3,4]

Results from multiple solder alloy studies indicate that In additions can improve drop and shock resistance by slowing the growth of interfacial IMC layers. Yu et al report improved drop [33] and thermal shock [34] performance by adding as little as 0.4% In, and Amagai et al report improved drop performance at or below 0.5 % In [35]. Hodúlová et al In slows growth of Cu<sub>3</sub>Sn and that a hybrid IMC phase Cu<sub>6</sub>(Sn, In)<sub>5</sub> forms [36]. Sharif also observed the formation of the Cu<sub>6</sub>(Sn, In)<sub>5</sub> IMC as well as formation of (Cu, Ni)<sub>3</sub>(Sn, In)<sub>4</sub> on Ni substrates [37], and these IMCs also could be found in the bulk as well as the interfaces. In these hybrid IMCs, In substitutes for Sn which fundamentally is different than the common modified IMCs (Cu, Ni)<sub>6</sub>Sn<sub>5</sub> or the (Ni, Cu)<sub>3</sub>Sn<sub>4</sub> where Cu and Ni exchange.

Other reactions can occur when In is added to SAC-based solders, and this complicates the ability to understand the effect of In content on solder joint reliability. In a study by Chantaramanee et al additions of 0.5% In or Sb in combination with In was found to promote formation of Ag<sub>3</sub>(Sn, In) and SnSb [38]. They reported that small precipitates reduced the Sn dendrite size by 28%, but they were unable to determine the relative influence of In versus Sb on this reaction. With alloys containing In of the order of 10%, Sopoušek et al found that some of the Ag<sub>3</sub>Sn transforms to Ag<sub>2</sub>(Sn, In) and Ag<sub>2</sub>Sn [39]. These observations are consistent with the Ag-Sn binary phase diagram that shows Ag<sub>3</sub>In, Ag<sub>2</sub>In, and AgIn,

[17]. Wang et al reported that an addition of 1% In caused larger or coarser Ag<sub>3</sub>Sn precipitates [40]. This is an interesting observation, since Ag<sub>3</sub>Sn precipitate coarsening (larger precipitates at time zero) could reduce thermal cycling reliability. In principle there is a large solid solubility of In in Sn, but the effective In content in a SAC-based solder may be diminished by interactions with other elements to form multiple phases.

It is noteworthy that many of the studies were conducted using laboratory bulk solder samples with microstructures that are likely to be atypical of microelectronic solder joints. Some of the studies also included more than one significant alloy addition [e.g., 38], which makes it difficult to isolate effects due to individual alloying elements. The work by Wada et al [31,32], while it includes tensile testing with comparatively large, bulk samples, also includes thermal cycling and drop testing with surface mount components. Their microstructural analysis included X-ray diffraction and they found InSn<sub>4</sub>, In<sub>4</sub>Ag<sub>9</sub>, Ag<sub>3</sub>(Sn, In), and possibly αSn in addition to βSn. Wada concluded that the optimum ductility and reliability was achieved with an In content of 6 wt. %.

# Bismuth (Bi) Additions to Tin (Sn)

The binary Sn-Bi phase diagram in shown in Figure 20. The solubility of Bi in Sn is approximately 1.5 wt. % at room temperature and increases to almost 7 wt. % at 100°C room temperature, and as much as 15 wt. % at 125°C [3,4]. There is almost no solubility of Sn in Bi, and no intermediate phases or IMC are found in the Sn-Bi system.

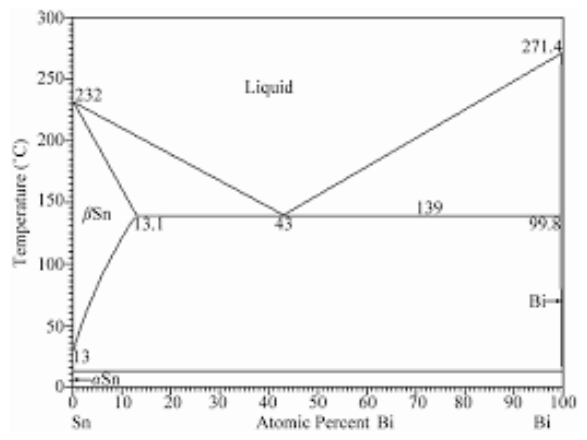


Figure 20: The Sn-Bi binary phase diagram [3,4]

Multiple studies have shown that Bi improves the mechanical properties of Sn and SAC solders [41, 18, 19, 42-54]. Vianco [42,43] and Witkin [46, 50-52] have done extensive mechanical testing and microstructural analysis and discuss the dual strengthening mechanisms of Bi in solid solution and Bi precipitated within Sn dendrites and at Sn boundaries. Recently, Delhaise et al [53] reported results from their study of the effects of thermal preconditioning (aging) on microstructure and property improvement in an alloy containing 6 wt. % Bi. They suggest that strain from Bi precipitation induces recrystallization and an increase in the amount of Sn grain boundaries which in turn, are pinned by the Bi precipitates at those

boundaries. These microstructural features work in conjunction with Bi in solid solution to resist creep deformation.

The results from the fundamental studies by Vianco [42,43] and Witkin [46, 50, 51] leave no doubt that Bi additions can have a positive effect on the physical properties of Sn and Sn-based solder alloys. However, those studies used cast, bulk alloy samples and it is debatable if those results can be scaled effectively to smaller, microelectronic solder joints. Nishimura et al for example, recommend a maximum Bi content of only 1.5 wt. % (Figure 21a) because of the uncertainly that the alloying effect will be sustained as the microstructure evolves in response to the thermal cycling in normal service [48]. Delhaise has shown that the Bi distribution and microstructure depend on solidification conditions and subsequent thermal exposure, which determine the relative contributions of Bi to solid solution and dispersion strengthening (Figure 21b).

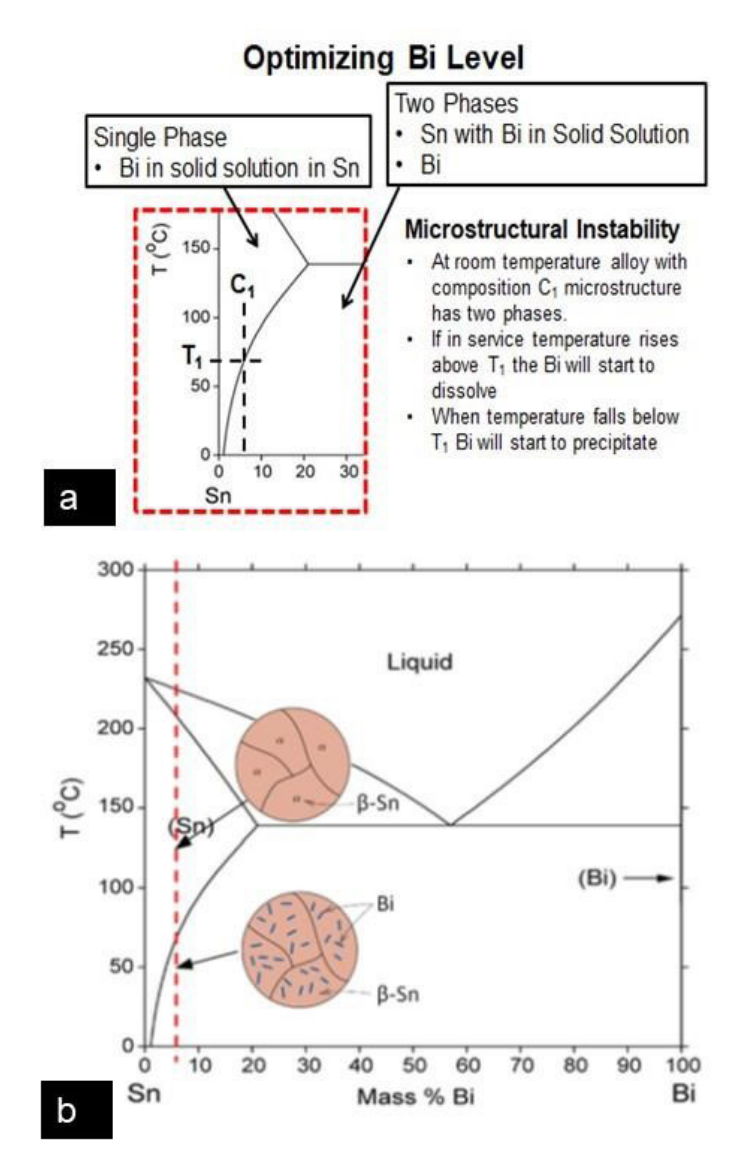


Figure 21: Emphasis on the Sn-rich regions of the Sn-Bi binary phase diagram showing: a) Factors to consider when for optimizing the Bi level, courtesy, K. Sweatman [54], and b) Microstructures shown schematically for solid solution (upper) and dispersion strengthening (lower) with the 6 wt. % Bi alloy (Violet), from Delhaise [53].

Furthermore, it is possible that adding enough Bi to take advantage of the Bi solubility limit at higher temperatures may have a negative effect because Bi does not always precipitate homogeneously. Clustering of Bi is known to occur [53] and in the extreme case, stratification or segregation may induce brittle behavior [55,56]. The current experimental test plan offers the opportunity to explore the stability of the Bi content in the 6 wt. % Bi alloy (Violet) alloy using thermal cycling at upper temperature extremes of 100 °C and 125 °C.

These intermetallic precipitates are recognized as the primary strengthening mechanism in SAC solders [57, 58, 42, 43]. During thermal or power cycling and extended elevated temperature exposure, the Ag<sub>3</sub>Sn precipitates coarsen and become less effective in inhibiting dislocation movement and slowing damage accumulation. This pattern of microstructural evolution is characteristic of the thermal fatigue failure process in these Sn-based Pb-free alloys and was described originally in detail by Dunford et al in 2004 [20]. Figure 8 shows scanning electron micrographs illustrating coarsening of the Ag<sub>3</sub>Sn precipitates in SAC305 solder caused by thermal cycling.

### **DISCUSSION**

It would be incorrect to state that the various IMC phases described in the paper are not associated with solder joint reliability issues. However, the emphasis on the impact of IMC phases on solder joint is clearly overstated in the electronic industry. The following five case studies document validated IMC defect root cause examples.

# Case #1: Literature Investigations

The authors review 1, 549 papers in the Journal of Electronic Materials and 951 papers in the IEEE Xplore publication databases looking for publications on product or field failures relating to IMC phases are the failure root cause. Only two published papers were found: (1) C. Lim et al., "Failure Characterization of BGA Solder Joint Fracture During Field Application" which concluded the solder joint failure was due to excessive IMC thickness due to multiple reflow cycles [59]; (2) Y. Mo et al., "Failure Analysis on the BGA Solder Joint" which concluded that the solder joint failure was due to irregular 25.75 um IMC thickness [60].

# Case #2: Microcracking of Copper/Tin IMC Phases Impacting Specific Product Applications

Hodolova et al found that the Cu<sub>6</sub>Sn<sub>5</sub> IMC phase developed micro-cracks at the IMC phase after oven thermal aging from 130C - 170C for 2-16 days and thermal cycle conditioning [7]. These micro-cracks illustrated brittleness of the IMC phase, but overall degradation of the solder joint would require significant mechanical deformation. Their work also demonstrated that the constituent additions of bismuth and indium impacted the IMC phase growth rates and decreased the overall rated of IMC phase micro-cracking. Similarly, K Sweatman et al, investigated the influence of nickel and reflow profile parameters on the microcracking of the Cu<sub>6</sub>Sn<sub>5</sub> IMC phase [61,62]. The microcracking observed in the solder joints would not be considered a major reliability issue but could pose a

solder joint cracking risk in certain specific commercial product applications.

# Case #3: Assembly Failure Due to Improper Maintenance

The introduction of SAC soldering processes resulted in significant changes to wave solder and selective solder equipment due to the increased dissolution properties of SAC solder in comparison to SnPb solder. The solder pots containing the molten SAC solder alloy required either a protective coating or be constructed of a dissolution resistant metal such as titanium. Solder pots made from iron-based metals could be significantly damaged due to dissolution of the iron by the molten solder resulting in the formation of iron/ tin IMC needle-like structures. A review of the iron/tin phase diagram shows that two intermetallic compounds (IMCs) can be formed – FeSn or FeSn, which are not wettable by solder. D. Barbini [63] documented the formation of FeSn, IMC structures due to the increased dissolution capacity of lead-free solders. FeSn, IMC structures have a higher density than molten tin/lead or lead-free solder; therefore, if they form, they will sink to the bottom of a wave solder pot, which results in their accumulation and damage to the wave solder pot impellers without proper maintenance. Figure 22 illustrates a wave solder pot accumulation of FeSn, IMC structures. Manko [64], Schlessmann [65], and Diepstraten & Trip [66] all documented similar formations of FeSn, IMC structures due to dissolution of iron from a wave solder pot.

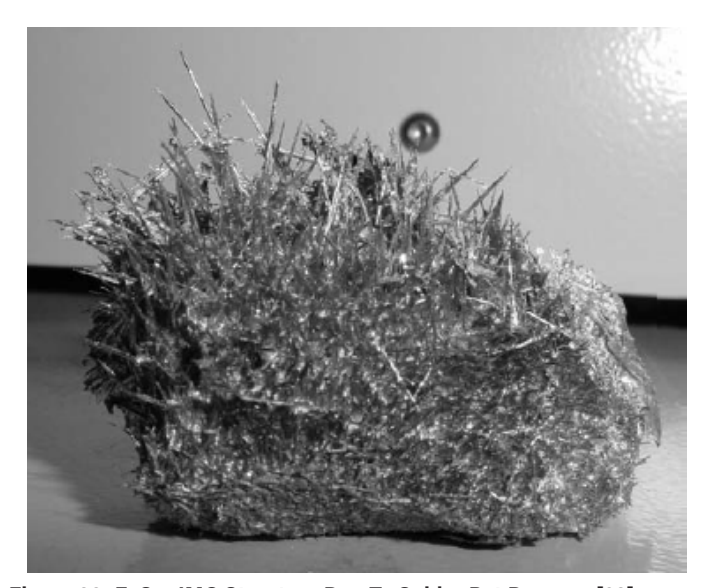


Figure 22: FeSn<sub>2</sub> IMC Structure Due To Solder Pot Damage [63]

Cookson Electronics documented an identical analysis of FeSn<sub>2</sub> IMC due to excessive preventative maintenance of a tin/lead wave solder process [67]. Overly aggressive scrapping of the wave solder pot during dross removal was found to have damaged the wave solder pot protective coating, which allowed for the dissolution of iron and the formation of the FeSn<sub>2</sub> IMCs. The FeSn<sub>2</sub> IMC structures were then transferred by the molten solder forming bridged solder joints on printed wiring assemblies (see Figure 23).

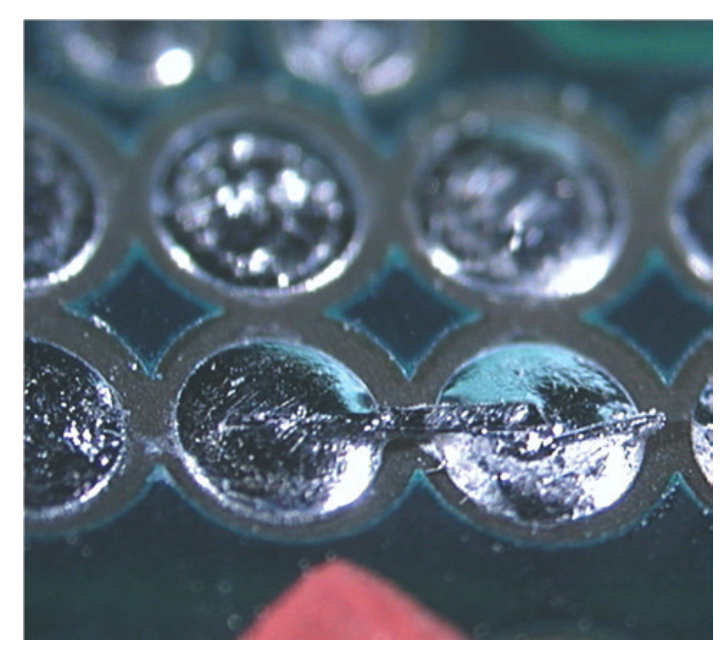


Figure 23: FeSn<sub>2</sub> IMC Phase Solder Defect [67]

Improper maintenance of SnPb wave solder and selective solder equipment is not immune from the possible impact of FeSn<sub>2</sub> IMC phase defects. Figure 24 illustrates a similar defect root cause for a SnPb wave solder system where the FeSn<sub>2</sub> IMC phase formation resulted in the shorting of solder joints [6]. Scanning electron microscopy identified the IMC phase as FeSn<sub>2</sub> (Figure 25).

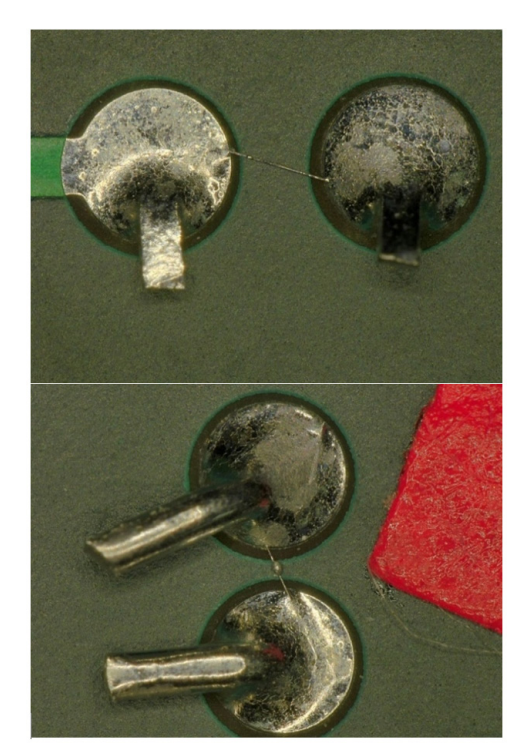


Figure 24: FeSn, IMC Phase Shorting Defect

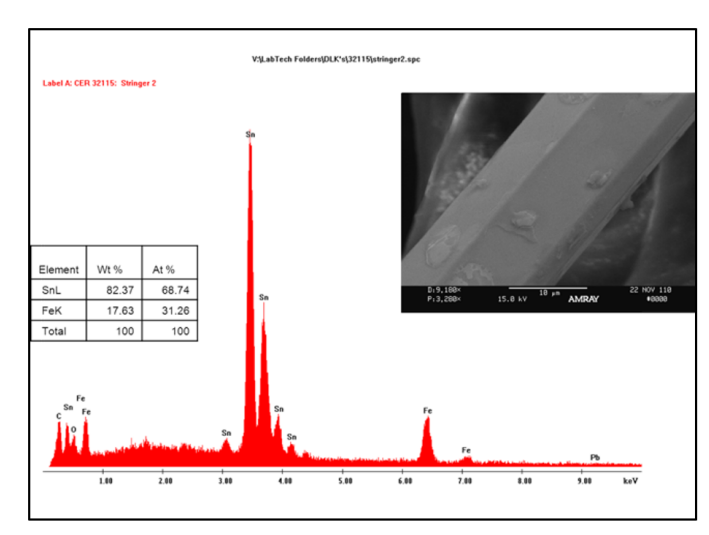


Figure 25: SEM Identification of the IMC Phase as FeSn,

# Case #4: Tin/Copper IMCs Masquerading as Tin Whiskers - Inadequate Tinning Pot Protocols

The implementation of the Restriction of Hazardous Substances (RoHS) European Union (EU) Directive in 2005 resulted in the introduction of pure tin as an acceptable surface finish for printed circuit boards and component terminations. A drawback of pure tin surface finishes is their potential to form tin whiskers. The tin whisker metallurgical phenomenon is associated with tin rich/pure tin materials and has been a topic of intense industry interest [68-73]. Figure 26 illustrates tin whiskers observed on a component lead and in an immersion tin surface finished plated through hole that was incorrectly plated.

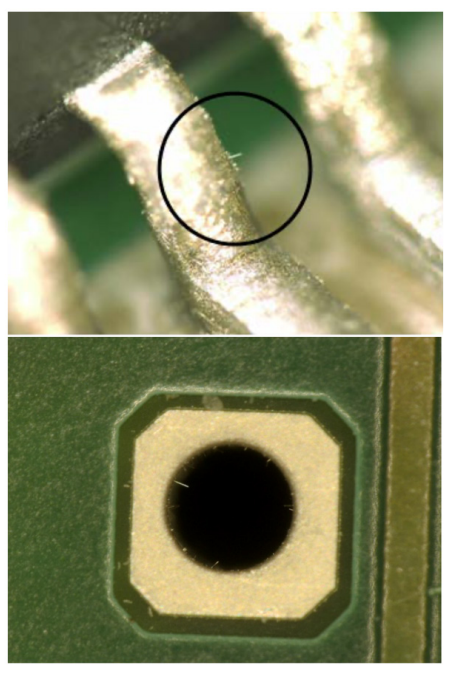


Figure 26: Tin Whiskers Observed on a Component Lead (top) and in a Plated Through Hole (bottom) [74]

As previously discussed, SnPb soldering processes result in the formation of the Cu<sub>6</sub>Sn<sub>5</sub> IMC phase which can be observed distributed around the solder joint microstructure as needles. The Cu<sub>6</sub>Sn<sub>5</sub> intermetallic needles have a hollow, hexagonal geometry. One industry failure analysis documented a case of mistaken identity of tin whiskers and copper/tin IMCs. The inspection of a printed circuit assembly revealed tin whiskers on a quad flat pack (QFP) component (Figure 27).

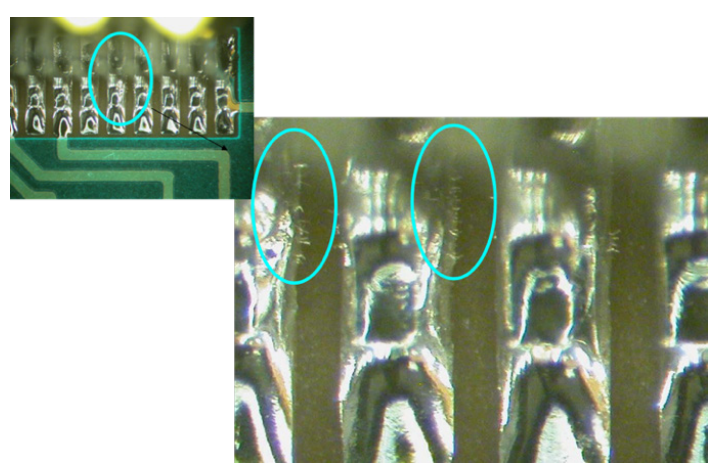


Figure 27: Observed Structures on QFP Component

Scanning electron microscopy (SEM) analysis results revealed the identity of the whisker-like anomalies observed on the QFP component. The SEM EDX results show a copper/tin element ratio of the anomalies to be approximately six parts copper to five parts tin which would correspond to the Cu<sub>2</sub>Sn<sub>5</sub> tin/copper IMC phase [75]. The Cu<sub>2</sub>Sn<sub>5</sub> tin/copper IMC phase forms in a needle morphology as the copper content of the solder begins to exceed approximately 0.3% [76, 1]. The Cu<sub>2</sub>Sn<sub>5</sub> intermetallic needles often form and grow preferentially from component lead and/or printed wiring pad edges. Figures 28 and 29 illustrate the QFP defects observed during SEM analysis. A review of the QFP component history revealed that QFP component was not placed during automated assembly process due to a lack of QFP component availability. The QFP was manually soldered by an operator. Further investigation of the operator's QFP soldering procedure did not reveal any unusual or incorrect soldering technique or procedure. It is hypothesized that original QFP tin/lead surface finish contained higher than normal copper content and the manual soldering operation resulted in the formation of the Cu<sub>e</sub>Sn<sub>5</sub> tin/ copper intermetallic needles. A solder wick and re-soldered process was conducted on QFPs that exhibited the Cu<sub>s</sub>Sn<sub>e</sub> tin/copper intermetallic needles and no reoccurrence of the Cu<sub>c</sub>Sn<sub>5</sub> tin/copper intermetallic needles was observed after completion of the process.

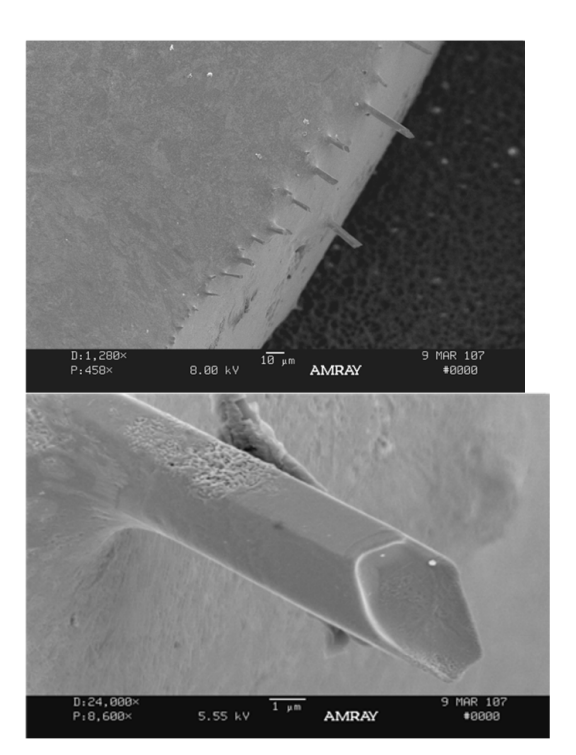


Figure 28: Scanning Electron Microscopy Image of  $\mathrm{Cu_eSn_5}$  IMC Phase As Soldered

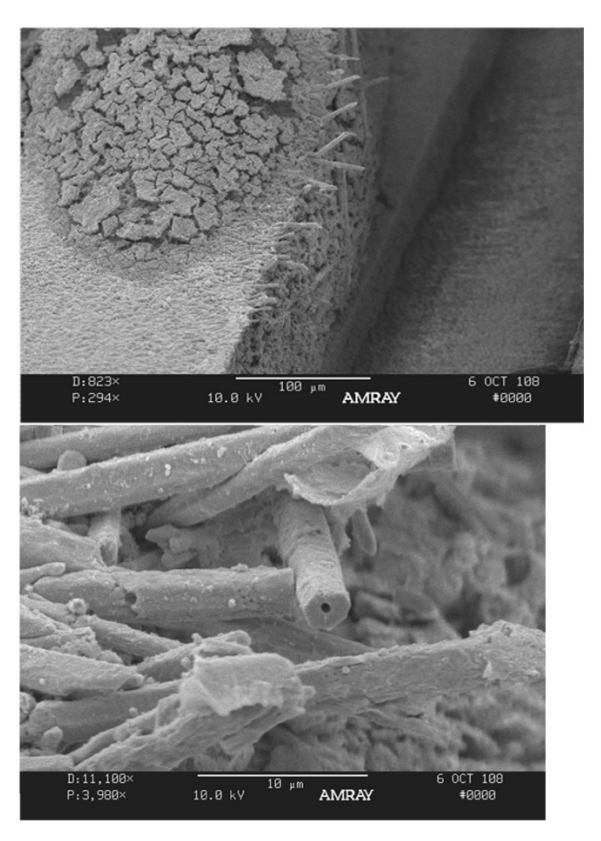
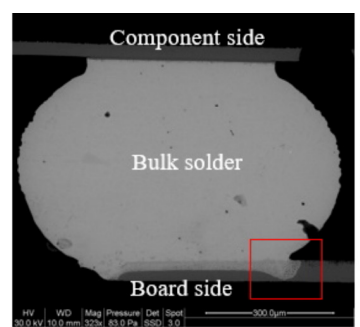


Figure 29: Scanning Electron Microscopy Image of  $\mathrm{Cu_6Sn_5}$  IMC Phase After Etching

# Case #5: Improper Rework Processes Impacting Copper/ Tin IMC Phases

Excessive IMC phase formation is typically the result of improper soldering or rework/repair processes. Excessive soldering temperatures or soldering dwell times allows the formation of thick IMC phase thicknesses at the expense of the printed circuit board component pad. Figure 30 illustrates the impact of five rework operations on a BGA component resulting in the excessive copper/tin IMC and dissolution of the BGA pad. Figure 31 illustrates a more severe case of BGA improper rework where the component copper pad is nearly eliminated due to dissolution by the SAC solder alloy. The severe damage to the component copper pad could result in solder joint cracking, pad cracking or pad delamination from the printed circuit board laminate under mechanical stress or fatigue conditions.



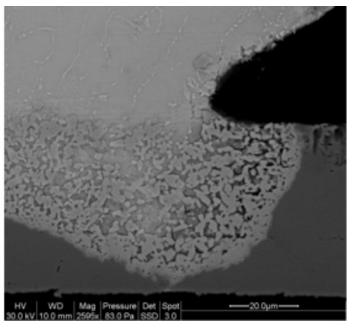


Figure 30: Excessive Copper/Tin IMC Formation At BGA Copper Pad After 5 Rework Operations [Photos courtesy of CALCE]



Figure 31: Excessive BGA Component Rework Resulting In Near Complete Pad Dissolution/Excessive IMC [77]

The electronics industry focus on the IMC phases/IMC thicknesses results in misinterpretation of solder joint failures and root cause corrective action. The root causes of the discussed detailed cases revealed a wide range of issues: improper maintenance, excessive rework procedures, inadequate tinning pot protocols, specific high strain commercial product application and incorrect/inadequate

soldering processes. The industry emphasis should be on better soldering processes, rigidly controlled rework protocols and detailed focus failure analysis. The industry data demonstrates that brittle IMC phases should not be a primary concern for solder joint reliability. Vianco's summary of the influence of the IMC phase on solder joint reliability is a perfect summary: "..the propensity for failure to occur in the IMC layer depends upon the following factors: (1) the strength of the solder alloy; (2) the rate at which a load is applied to the joint (relating to the strain rated sensitivity of the solder alloy); (3) the brittleness of the IMC layer composition; (4) the thickness of the IMC layer." [1]. Over emphasis of IMC phase as a s primary older joint reliability issue only consumes cost/time resources with no contribution of problem resolution.

# **CONCLUSION**

The emphasis on the influence of IMC phases on solder joint reliability in the electronics industry is clearly overstated and often excessive. A review of industry publications/cases clearly shows that solder joint reliability is impacted by IMC phases with root causes of incorrect soldering processes or inadequate process procedure. The list of solder joint reliability root cause failures should not include IMC phases as a primary solder joint failure mode.

# **REFERENCES**

- 1. P. Vianco, Soldering Handbook, 3rd Edition, American Welding Society, ISBN 0-87171-618-6
- 2. P. Ratchev et al, "A Study of Ductile to Brittle Fracture Transition Temperatures in Bulk Pb free Solder Alloys," EMPC 2005, Brugge, Belgium
- 3. Max Hansen, Constitution of Binary Alloys, 2nd edition, McGraw-Hill, 1175-1177, 1958.
- 4. Rodney P. Elliot, Constitution of Binary Alloys, First Supplement, McGraw-Hill, 802, 1965.
- 5. P. Vianco, et al, Solid State Intermetallic Compound Layer Growth Between Copper and SAC Solder," Journal of Electronic Materials, Vol. 33, No. 9, September 2004]
  - 6. D.Hillman, unpublished manuscript
- 7. E. Hodulova, et al, "Structural Changes of the IMC in Lead Free Solder Joints," Materials Transactions, Vol. 56, No. 7, 2015.
- 8. R. Coyle et al., "The effect of bismuth, antimony, or indium on the thermal fatigue of high reliability Pb- free solder alloys," SMTA International Conference, 2018.
- 9. W. Bader, "Dissolution of Au, Ag, Pd, Pt, Cu, and Ni in a Molten Tin-Lead Solder," Welding Journal 48, 1969.
- 10. D. Hillman et al, "Dissolution Rate of Electronics Packaging Surface Finish Elements in Sn3.0Ag0.5Cu Solder", Journal of Electronic Materials, No. 48, 2019.
- 11. M. Bester, "Metallurgical Aspects of Soldering Gold and Gold Plating," InterNEPCON Proceedings, 1968.
- 12. I. Artaki et al, "Assessment of Nickel-Palladium Finished Components for Surface Mount Assembly Applications", SMTAI Conference Proceedings, 1995.
- 13. D. Hillman et al, "Wirebondability and Solderability of Various Metallic Finishes for Use in Printed Circuit Assembly, SMTAI Conference Proceedings, 1996.

14. A. Mei and A. Eslambolchi, "Evaluation of Ni/Pd/ Au as an Alternative Metal Finish on PCB", SMTAI Conference Proceedings, 1998.

- 15. D. Hillman et al, "JCAA/JGPP No-Lead Solder Project: -55C to +125C Thermal Cycle Testing Final Report", Navy Mantech Contract GST 0504BM3419-02, March 2006.
- 16. G. E. Dieter, Mechanical Metallurgy, Chapter 5, "Plastic Deformation of Polycrystalline Aggregates, Solid Solution Hardening," 128, McGraw-Hill, 1961.
- 17. Peter Haasen, Physical Metallurgy, 3 Edition, Cambridge University Press, 375-378, 1996.
- 18. Anton-Zoran Miric, "New Developments In High-Temperature, High-Performance Lead-Free Solder Alloys," SMTA Journal, Volume 23, Issue 4, 24-29, 2010.
- 19. André Delhaise, Leonid Snugovsky, Doug Perovic, Polina Snugovsky, and Eva Kosiba, "Microstructure and Hardness of Bicontaining Solder Alloys after Solidification and Ageing," SMTA J., Vol. 27, issue 3, 22-27, 2014.
- 20. S. Dunford, S. Canumalla, and P. Viswanadham, "Intermetallic Morphology and Damage Evolution Under Thermomechanical Fatigue of Lead (Pb)-Free Solder Interconnections," Proceedings of Electronic Components Technology Conference, 726-736, Las Vegas, NV, June 1-4, 2004.
- 21. "Lead-Free Solder Project Final Report," NCMS Report 0401RE96, Section 2.4, Properties Assessment and Alloy Down Selection, National Center for Manufacturing Sciences, Ann Arbor, MI, May 1997.
- 22. T. Siewert, S. Liu, D. R. Smith, and J. C. Madeni, "Database for Solder Properties with Emphasis on New Lead-Free Solders: Properties of Lead-Free Solders Release 4.0," NIST and Colorado School of Mines, February 2002.
- 23. C. A. Handwerker, U. Kattner, K. Moon, J. Bath, and P. Snugovsky, "Chapter 1, Alloy Selection," in Lead-Free Electronics, 9-46, IEEE Press, Piscataway, NJ, 2007.
- 24. Li, G.Y., Chen, B.L., Tey, J.N., "Reaction of Sn- 3.5Ag-0.7Cu-xSb solder with Cu metallization during reflow soldering," IEEE Transactions on Electronics Packaging Manufacturing, vol. 27, no. 1, 77-85, 2004.
- 25. Li, G.Y., Bi, X.D., Chen, Q., Shi, X.Q., "Influence of dopant on growth of intermetallic layers in Sn-Ag-Cu solder joints," Journal of Electronic Materials, vol. 40, no. 2,165-175, 2011.
- 26. Per-Erik Tegehall "Review of the Impact of Intermetallic Layers on the Brittleness of Tin-Lead and Lead-Free Solder Joints, Section 3, Impact of Intermetallic Compounds on the Risk for Brittle Fractures" IVF Project Report 06/07, IVF Industrial Research and Development Corporation, 2006.
- 27. Lu, S., Zheng, Z., Chen, J., Luo, F.," Microstructure and solderability of Sn-3.5Ag-0.5Cu-xBi-ySb solders," Proceedings 11th International Conference on Electronic Packaging Technology and High Density Packaging, ICEPT-HDP 2010, 410-412, 2010.
- 28. A.A. El-Daly, Y. Swilem and A.E. Hammad, "Influences of Ag and Au Additions on Structure and Tensile Strength of Sn-5Sb Lead Free Solder Alloy," J. Mater. Sci. Technol., vol.24, no. 6, 921-925, 2008.

- 29. H. Beyer, V. Sivasubramaniam, D. Hajas, E. Nanser, F. Brem, "Reliability improvement of large area soldering connections by antimony containing lead-free solder," PCIM Europe Conference Proceedings, 1069-1076, 2014.
- 30. A.A. El-Daly, Y. Swilem, A.E. Hammad, "Creep properties of Sn–Sb based lead-free solder alloys," Journal of Alloys and Compounds, vol. 471, 98-104, 2009.
- 31. T. Wada, K. Mori, S. Joshi, and R. Garcia, "Superior Thermal Cycling Reliability of Pb-Free Solder Alloy by Addition of Indium and Bismuth for Harsh Environments, Proceedings of SMTAI, 210-215, Rosemont, IL, Sep 2016.
- 32. T. Wada, S. Tsuchiya, S. Joshi, and R. Garcia, K. Mori, and T. Shirai, "Improving Thermal Cycle Reliability and Mechanical Drop Impact resistance of a Lead-free Tin- Silver-Bismuth-Indium Solder Alloy with Minor Doping of Copper Additive," Proceedings of IPC APEX, San Diego, CA, February 14-16, 2017.
- 33. A-M Yu, J-W Jang, J-H Lee, J-K Kim, M-S Kim, "Microstructure and drop/shock reliability of Sn-Ag-Cu-In solder joints," International Journal of Materials and Structural Integrity, vol. 8 no. 1-3, 42-52, 2014.
- 34. A-M Yu, J-W Jang, J-H Lee, J-K Kim, M-S Kim, "Tensile properties and thermal shock reliability of Sn-Ag- Cu solder joint with indium addition," Journal of Nanoscience and Nanotechnology, vol. 12, no. 4, 3655- 3657, 2012.
- 35. M. Amagai, Y. Toyoda, T. Ohnishi, S. Akita, "High drop test reliability: Lead-free solders," Proceedings 54th Electronic Components and Technology Conference, 1304-1309, 2004.
- 36. E. Hodúlová, M. Palcut, E. Lechovič, B. Šimeková, K. Ulrich, "Kinetics of intermetallic phase formation at the interface of Sn-Ag-Cu-X (X = Bi, In) solders with Cu substrate," Journal of Alloys and Compounds, vol. 509, no. 25, 7052-7059, 2011.
- 37. A. Sharif, Y. C. Chan, "Liquid and solid state interfacial reactions of Sn-Ag-Cu and Sn-In-Ag-Cu solders with Ni-P under bump metallization," Thin Solid Films, vol. 504, no. 1-2, 431-435, 2006.
- 38. S. Chantaramanee, P. Sungkhaphaitoon, T. Plookphol, "Influence of indium and antimony additions on mechanical properties and microstructure of Sn-3.0Ag-0.5Cu lead free solder alloys," Solid State Phenomena, 266 SSP, 196-200, 2017.
- 39. J. Sopoušek, M. Palcut, E. Hodúlová, J. Janovec, "Thermal analysis of the Sn-Ag-Cu-In solder alloy," Journal of Electronic Materials, vol. 39, no. 3, 312-317, 2010.
- 40. J. Wang, M. Yin, Z. Lai, X. Li, "Wettability and microstructure of Sn-Ag-Cu-In solder," Hanjie Xuebao/Transactions of the China Welding Institution, vol. 32, no. 11, 69-72, 2011.
- 41. Polina Snugovsky, Simin Bagheri, Marianne Romansky, Doug Perovic, Leonid Snugovsky, and John Rutter, "New Generation Of Pb-Free Solder Alloys: Possible Solution To Solve Current Issues With Mainstream Pb-Free Soldering," SMTA J., Vol. 25, issue 3, 42-52, July 2012.
- 42. P.T. Vianco and J.A. Rejent, "Properties of Ternary Sn- Ag-Bi Solder Alloys: Part I Thermal Properties and Microstructural Analysis," J. Electronic Materials, Vol. 28, no. 10, 1127-1137, 1999.

43. P.T. Vianco and J.A. Rejent, "Properties of Ternary Sn-Ag-Bi Solder Alloys: Part I - Wettability and Mechanical Properties Analyses," J. Electronic Materials, Vol. 28, no. 10, 1138-1143, 1999.

- 44. Jie Zhao,, Lin Qi, Xiu-min Wang, "Influence of Bi on microstructures evolution and mechanical properties in Sn– Ag–Cu lead-free solder," J. Alloys and Compounds, Vol. 375, Issues 1–2, 196-201, July 2004.
- 45. Dave Hillman, Tim Pearson, and Ross Wilcoxon, "NASA DOD -55 °C to +125 °C Thermal Cycle Test Results," Proceedings of SMTAI 2010, 512-518, Orlando, FL, October 2010.
- 46. David Witkin, "Mechanical Properties of Bi-containing Pb-free Solders," Proceedings IPC APEX 2013, S11-01, San Diego, CA, February 2013.
- 47. Joseph M. Juarez, Jr., Polina Snugovsky, Eva Kosiba, Zohreh Bagheri, Subramaniam Suthakaran, Michael Robinson, Joel Heebink, Jeffrey Kennedy, and Marianne Romansky, Manufacturability and Reliability Screening of Lower Melting Point Pb-Free Alloys Containing Bismuth, J. Microelectronics and Electronic Packaging," Vol. 12, no. 1, 1-28, 2015.
- 48. Takatoshi Nishimura, Keith Sweatman, Akira Kita, Shuhei Sawada, "A New Method of Increasing the Reliability of Lead-Free Solder, Proceedings of SMTAI 2015, 736-742, Rosemont, IL, October 2015
- 49. A. Delhaise, L. Snugovsky, D. Perovic, P. Snugovsky, E. Kosiba, The Effects of Bi and Ageing on the Microstructure and Mechanical Properties of Sn-rich Alloys, Pt. 2, 2016 International Conference on Soldering & Reliability, Toronto, Canada, May 9-11, 2016.
- 50. David Witkin, Mechanical Properties of Bi-containing Pb-Free Solders, APEX Expo 2013, San Diego, CA, February 16-21, 2013
- 51. David Witkin, "Creep Behavior of Bi-Containing Lead-Free Solder Alloys," Journal of Electronic Materials, vol. 41, no. 2, 190-203, 2012.
- 52. David B. Witkin, "Influence of microstructure on quasistatic and dynamic mechanical properties of bismuth- containing lead-free solder alloys,", Materials Science and Engineering A, vol. 532, 212-220, 2012.
- 53. André M. Delhaise, Polina Snugovsky, Ivan Matijevic, Jeff Kennedy, Marianne Romansky, David Hillman, David Adams, Stephan Meschter, Joseph Juarez, Milea Kammer, Ivan Straznicky, Leonid Snugovsky, Doug D. Perovic, "Thermal Preconditioning, Microstructure Restoration and Property Improvement in Bi-Containing Solder Alloys," SMTA Journal, vol. 31, issue1, 33-42, 2018
- 54. Keith Sweatman, Nihon Superior, private communication, November 2017.
- 55. C. H. Raeder, L. E. Felton, D. B. Knott, G. B. Shmeelk and D. Lee, "Microstructural Evolution and Mechanical Properties of Sn-Bi based Solders," Proceedings of International Electronics Manufacturing Technology Symposium, 119-127, Santa Clara, CA, October 1993.

- 56. Richard Coyle, Raiyo Aspandiar, Michael Osterman, Charmaine Johnson, Richard Popowich, Richard Parker, Dave Hillman, "Thermal Cycle reliability of a Low Ag Ball Grid Array Assembled with Tin Bismuth Solder paste," Proceedings of SMTAI, 108-116, Rosemont, IL, September 17-21, 2017.
- 57. Richard Coyle, John Osenbach, Maurice Collins, Heather McCormick, Peter Read, Debra Fleming, Richard Popowich, Jeff Punch, Michael Reid, and Steven Kummerl, "Phenomenological Study of the Effect of Microstructural Evolution on the Thermal Fatigue Resistance of Pb-Free Solder Joints," IEEE Trans. CPMT, Vol. 1, No. 10, 1583- 1593, October 2011.
- 58. S. Terashima, Y. Kariya, Hosoi, and M. Tanaka, "Effect of Silver Content on Thermal Fatigue Life of Sn- xAg-0.5Cu Flip-Chip Interconnects," J. Electron. Mater. vol. 32, no. 12, 2003.
- 59. C. Lim etal, "Failure Characterization of BGA Solder Joint Fracture During Field Application," 12th Electronics Packaging Technology Conference, December 2010.
- 60. Y. Mo etal "Failure Analysis on the BGA Solder Joint," EEE Circuits and Systems International Conference on Testing and Diagnosis Conference, 2009.
- 61. K. Sweatman, et al, "Reducing Cracking in Solder Joint Interfacial Cu6Sn5 with Modified Reflow Profile", Transactions of The Japan Institute of Electronics Packaging Vol. 13, 2020.
- 62. K. Sweatman, et al, "The Role of Nickel in Solder Alloys Part 2. The Effect of Ni on the Integrity of the Interfacial Intermetallic in Sn-Based/Cu Substrate Solder Joints," SMTAI Conference, 2018.
- 63. D. Barbini, "Implementation of Lead-free Wave Soldering Process: An In-depth Look at the Critical Issues," SMTA Pan Pacific Conference Proceedings, 2005.
- 64. H. Manko, Solders and Soldering, ISBN 0-07-039970-0, McGraw Hill, 1992, 3rd Edition.
- 65. H. Schlessmann, "Lead-Free Technology and the Necessary Changes in Soldering Process and Machine Technology," IPC APEX Conference Proceedings, Session S4-01, 2002.
- 66. G. Diepstraten & H. Trip, "How to manage wave solder alloy contaminations," IPC Midwest Conference presentation, 2011.
- 67. Cookson Electronics, CE Analysis Case Study #6, On-line Report.
- 68. D. Hillman, et al, "JCAA/JG-PP No-Lead Solder Project: -55°C to +125°C Thermal Cycle Testing Final Report", Rockwell Collins Working Paper WP06-2021, October 2006.
- 69. Tin Whiskers: A History of Documented Electrical System Failures, A Briefing Prepared for the Space Shuttle Program Office, Dr. Henning Leidecker/NASA Goddard, Jay Brusse/QSS Group, Inc. April 2006.
- 70. Evaluation of Conformal Coatings for Future Spacecraft Applications, B.D. Dunn, European Space Agency document ESA SP1173, August 1994.
- 71. GEIA-STD-0005-2, Standard for Mitigating the Effects of Tin Whiskers in Aerospace and High Performance Electronic Systems, Section C.2.2.4 Conformal Coat or Foam Encapsulation Over Whisker Prone Surfaces, Government Electronics and Information Technology Association (GEIA), June 2006.

72. Website: http://nepp.nasa.gov/WHISKER/experiment/exp2/index.html#current.

- 73. Tin Whisker Risk Factors, David Pinsky, Michael Osterman, and Sanka Ganesan, IEEE Transaction on Components and Packaging Technologies, Vol. 27, No. 2, June 2004.
- 74. D. Hillman et al, "The Influence of Element Lead (Pb) Content in Tin Plating on Tin Whisker Initiation/Growth," Journal of SMT, Vol. 36, Issue 1, 2023.
- 75. ASM Metals Handbook, Metallography, Structures and Phase Diagrams, Volume 8, 8th Edition, 1973.
- 76. R. Klein Wassink, Soldering In Electronics, ISBN 0-901150-24-X, Electrochemical Publications Limited, 1989.
  - 77. Milea Kammer/T. Pearson, private communication.

# **BIOGRAPHIES**



David D. Hillman is a Metallurgical Engineer in the Advanced Operations Engineering Department of Rockwell Collins Inc. in Cedar Rapids, Iowa. Mr. Hillman graduated from Iowa State University with a B.S. (1984) and M.S. (2001) in Material Science & Engineering. In his present assignment he serves as a consultant to

manufacturing on material and processing problems. He served as a Subject Matter Expert (SME) for the Lead-free Manhattan Project in 2009. He has published 200+ technical papers. Mr. Hillman was named a Rockwell Collins Fellow in 2016. He was named an IPC Raymond E. Prichard Hall of Fame award recipient in 2018. He serves as the Chairman of the IPC JSTD-002 Solderability committee. Mr. Hillman served as a Metallurgical Engineer at the Convair Division of General Dynamics with responsibility in material testing and failure analysis prior to joining Rockwell. He is a member of the American Society for Metals (ASM), the Minerals, Metals & Materials Society (TMS), and Surface Mount Technology Association (SMTA) and the Institute for Interconnecting and Packaging of Electronic Circuits (IPC).



Tim Pearson is a Materials and Process Engineer in the Advanced Operations Engineering department of Collins Aerospace in Cedar Rapids, Iowa. Mr. Pearson graduated from Iowa State University with a BS in Materials Science and Engineering. Tim began his career as a Thin Films Engineer at Texas Instruments in

a 300mm wafer fab. Tim has been working for Collins Aerospace (formerly Rockwell Collins) since 2015. In his current role, he helps develop new manufacturing processes, troubleshoots production issues, and does root cause analysis of failures related to soldering. He is a member of SMTA and IPC.



Richard Coyle is a Consulting Member of the Technical Staff in the Reliability Engineering organization of Nokia in Murray Hill, NJ. He is responsible for evaluating the reliability and quality of electronic assemblies in the Bell Labs Interconnection Failure Analysis Lab. He received his Ph.D. in Metallurgical Engineering

and Materials Science from the University of Notre Dame. He is a member of TMS, ASM International, the EPS of IEEE, IMAPS, SMTA, and AWS. He is Co-Conference Director of SMTAI and a past member of the Board of Directors of SMTA (VP of Technical Programs). He is on the Board of Directors of iNEMI and an iNEMI Fellow.